EPJ Web of Conferences **242**, 03003 (2020) https://doi.org/10.1051/epjconf/202024203003
FPY 2019

Using CGMF to estimate corrections for fission yields measured via γ-ray spectroscopy

P. Jaffke[1,2,*], *P.* Talou[3], *M.* Devlin[4], and *N.* Fotiades[4]

[1]System Evaluation Division, Institute for Defense Analyses, Alexandria, VA 22311, USA
[2]Theoretical Division, Los Alamos National Laboratory, Los Alamos, NM 87545, USA
[3]XCP-5, Computational Physics Division, Los Alamos National Laboratory, Los Alamos, NM 87545, USA
[4]Physics Division, Los Alamos National Laboratory, Los Alamos, NM 87545, USA

Abstract. Fission product yields have been inferred using γ-ray spectroscopy for several decades. Typically, these efforts have focused on even-Z even-A fission products as their nuclear structure are less complicated. To further simplify the situation, it is often assumed that no side-feeding to the ground-state occurs and multiplicity cuts have a negligible effect on the inferred yields. Using `CGMF`, a Hauser-Feshbach statistical decay model for the primary fission fragments, we estimate the impact of these assumptions and determine corrections for specific fission product yields. We report on these corrections and investigate their sensitivity to various nuclear parameters, specifically the spin distribution of the fission fragments and the assumed nuclear structure. Our results indicate that even in the simplest of cases, say the $2^+ \rightarrow 0^+$ transitions in even-Z even-A fragments, average level corrections are on the order of 75%.

1 Introduction

Gamma-ray spectroscopy has been utilized to infer fission yields for a variety of nuclear reactions [1–4]. Experimental efforts have spanned prompt γ-ray emission times from within 1 μs or so [5, 6] to emissions after β-decays in the days to months range [7, 8]. Prompt γ-ray emissions are sensitive to the independent fission product yields (i.e. prior to β-decays), while later γ-ray emissions after β-decay are more sensitive to cumulative yields. Here we focus on γ-ray emissions prior to 150 ns.

Often, experimental assumptions and corrections must be applied to the data in order to properly account for energy resolution, nuclear transition strengths, and multiplicity cut effects. In particular, for prompt γ rays, fission products are generated with a distribution in excitation energy and spin. This distribution further complicates the necessary corrections. In this work, we present preliminary calculations of three potential corrections required for prompt γ-ray spectroscopy and outline a procedure for a given experimental setup.

The three considered corrections are dubbed the purity ϵ_P, level ϵ_L, and multiplicity ϵ_M corrections. The purity correction stems from γ-ray transitions of similar energy to the desired transition being included in the finite energy bin of a given γ-ray spectroscopy detector.

*e-mail: pjaffke@ida.org

The level correction originates from the branching ratios of the different emissions. The multiplicity correction arises when experimental cuts are applied to either reduce the data rate or provide more assurance of a fission coincidence.

In Sec. 2, we describe the Hauser-Feshbach de-excitation model, which is used to estimate the needed corrections. Next, in Sec. 3, we detail the three specific corrections related to prompt γ-ray spectroscopy. In Sec. 4, the results are presented to illustrate the impact of using the corrections. Lastly, we conclude in Sec. 5.

2 Hauser-Feshbach de-excitation

Fission fragments are de-excited with a Monte Carlo statistical decay following the theory of Hauser and Feshbach [9]. This implementation is given by the `CGMF` [10] code, described in detail in Ref. [11]. The de-excitation begins with a provided distribution of fission fragments

$$Y(A, Z, \mathrm{TKE}, J^\pi) = Y(A) \times Y(\mathrm{TKE}|A) \times Y(Z|A) \times P(J^\pi|A, Z, U). \tag{1}$$

In Eq. 1, the fission fragment yield in mass A, charge Z, total kinetic energy TKE, and spin-parity J^π is given by $Y(A, Z, \mathrm{TKE}, J^\pi)$. In the calculations presented here, we utilize fits to experimental data for the $^{235}\mathrm{U}(n_{\mathrm{th}}, f)$ reaction. A global fit is applied to $Y(A)$ and $Y(\mathrm{TKE}|A)$ experimental data, as done in Ref. [12], while the $Y(Z|A)$ is given by the Wahl systematics [13].

First, yields are sampled for a given fission event from Eq. 1 and the total excitation energy TXE is calculated via energy conservation $Q = \mathrm{TKE} + \mathrm{TXE}$. The Q-value is determined from nuclear masses [14], the incident neutron energy, and the binding energy. Next, the TXE is shared between the two fragments with a ratio of temperatures R_T, given by

$$R_T^2 = \frac{T_l^2}{T_h^2} \approx \frac{U_l a_h}{U_h a_l}, \tag{2}$$

where T_i is the nuclear temperature, U_i is the excitation energy, and a_i is the level density parameter for the light or heavy fragment. The use of Eq. 2 implicitly assumes the fragments are produced with sufficient excitation energy such that the level density is well-represented by a Fermi-gas model. In `CGMF`, we use a mass-dependent $R_T \equiv R_T(A)$, where the value of $R_T(A)$ is determined from fits to experimental $\bar{\nu}(A)$ data [15].

Next, the spin-parity distribution is sampled on an event-by-event basis. In `CGMF`, a spin-cutoff distribution $P(J^\pi)$ is used

$$P(J^\pi) = N(2J+1)\exp\left[\frac{-J(J+1)\hbar^2}{2\alpha T \mathcal{I}_0(A,Z)}\right], \tag{3}$$

where $\mathcal{I}_0(A, Z)$ is the moment of inertia for a rigid rotor, using the ground-state deformations of Ref. [14]. The factor N is a normalization factor and α is a spin scaling factor used to control the competition between γ-ray and neutron emission. For the calculations presented here, we use $\alpha = 1.45$ for $^{235}\mathrm{U}(n_{\mathrm{th}}, f)$. In `CGMF`, we assume an equal probability of parities and assume even(odd)-A fragments have even(odd)-J spin. Figure 1 illustrates the distribution of the primary fragments (i.e. prior to neutron emission) in blue for ^{100}Zr from the $^{235}\mathrm{U}(n_{\mathrm{th}}, f)$ reaction. The curve denotes using Eq. 3 and provides a good representation of the sampled distribution (points). The orange is the combined distribution from all events resulting in ^{100}Zr as a fission product (i.e. after prompt neutron emission). The neutron emission itself does not remove significant angular momentum, so a linear combination of Eq. 3 can be constructed to provide a reasonable estimation of the sampled points.

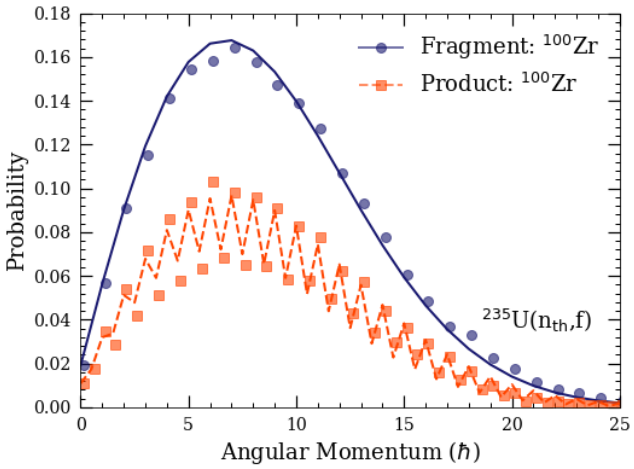

Figure 1. (Color online) Spin distribution of CGMF events initially sampling a ^{100}Zr fragment (in blue) and events resulting in a ^{100}Zr product after prompt neutron emission (in orange). Points denote the calculated distributions by CGMF, while the lines utilize Eq. 3. For the resulting product, a linear combination of $P(J)$ weighted by the prompt neutron emission is used to determine the total $P(J)$. Results are for ^{235}U(n_{th}, f) and one million events.

Now that an initial distribution $Y(A, Z, U, J^{\pi})$ has been established using Eqs. 1–3, the de-excitation can be determined through the calculation of transmission coefficients for γ-ray and neutron emission. As this process has been well-documented before [10, 11], we only summarize here. In CGMF, neutron transmission coefficients are determined using an optical model calculation with a global optical potential from Ref. [16]. Gamma-ray transmission coefficients follow the strength-function formalism of Ref. [17], with parameters from the Reference Input Parameter Library (RIPL-3) [18]. Discrete levels and their branching ratios are also from RIPL-3. The level densities follow the Gilbert-Cameron [19] form, with energy-dependent level density parameters via Ref. [20].

3 Corrections for prompt γ rays

Several calculations were conducted to estimate the effect of nuclear data and the spin scaling factor α on the determined corrections. The first calculation uses the 'optimal' spin scaling factor α discussed above and the improved 2015 RIPL-3 database. The second calculation supplements RIPL-3 with discrete level data for ^{104}Zr [21] and ^{138}Te [22, 23]. The third calculation increases the spin scaling factor α by about 10%. All calculations use one million events. Next, we detail the three corrections considered for prompt γ-ray spectroscopy.

The purity correction ϵ_P accounts for γ rays, both discrete and continuum transitions, mistakenly being counted in the photopeak of the target γ-ray energy E_γ. This quantity is determined by collecting all CGMF fission events containing γ rays with energy $E_\gamma \pm \delta(E_\gamma)/2$, where $\delta(E_\gamma)$ is a typical energy resolution of a Ge detector [24]. The fraction of those events that are actually emitted from the target fission product is given by ϵ_P. An example for several even-Z even-A fission products of ^{235}U(n_{th}, f) are given in the left-hand plot of Fig. 2.

The level correction ϵ_L accounts for the branching ratios and, implicitly, the distribution in excitation energy and spin-parity. For this quantity, we mask on all CGMF events that generated the target fission product. Next, we determine the fraction of this subset that actually

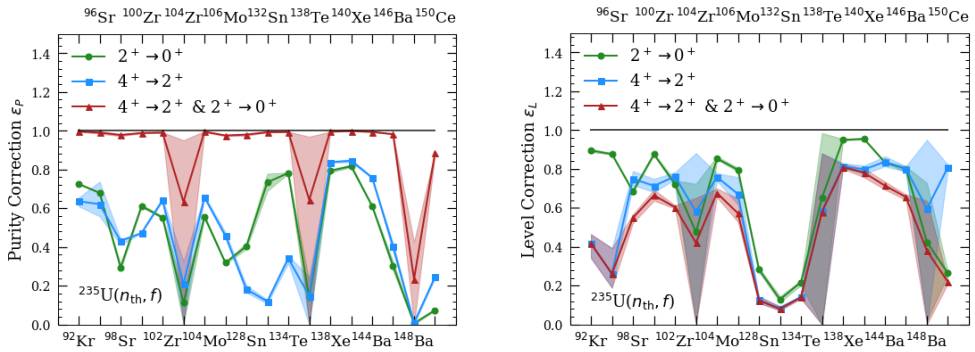

Figure 2. (Color online) Left plot shows the purity correction ϵ_P, while the right plot shows the level correction ϵ_L ratio for several even-Z even-A fission products. Circles (green) indicate the $2^+ \rightarrow 0^+$ transition, squares (blue) indicate the $4^+ \rightarrow 2^+$ transition, and triangles (red) indicate a double-gate on both. The curves and points signify the mean correction over the three CGMF calculations (see text). The bands show the upper and lower correction values, where bands that have a lower bound of zero indicate that the particular γ-ray transition did not exist in the default RIPL-3 database.

produced the target γ-ray transition E_γ. It is commonly assumed that for even-Z even-A fission products the $2^+ \rightarrow 0^+$ transition *always* occurs. In the right-hand plot of Fig. 2, we show that this is typically not the case. Rather, the median value is closer to 75%.

We note two significant findings from Fig. 2 here. First, the corrections depend on both the included nuclear data and the spin scaling factor α. Second, the corrections depend on the specific fission product transition greatly. Another significant finding, not displayed in Fig. 2, is that the corrections depend on the fission reaction, especially ϵ_P which is sensitive to the yields. Thus, it is important to realize that the exact corrections presented here are specific

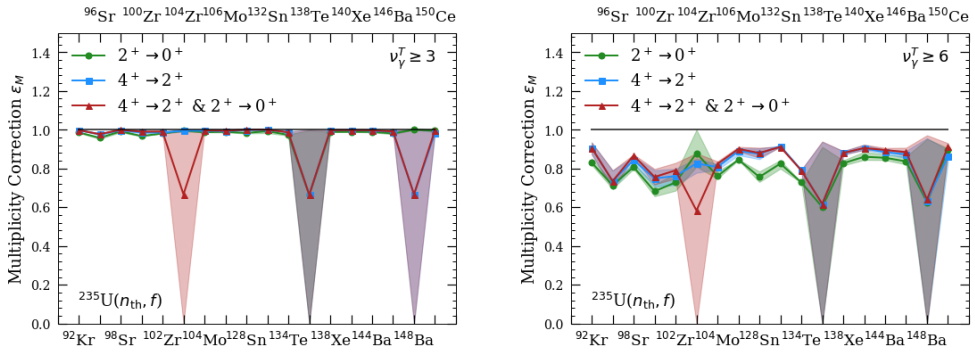

Figure 3. (Color online) Multiplicity correction ratio ϵ_M for $\nu_\gamma^T \geq 3$ (left) and $\nu_\gamma^T \geq 6$ (right) for several even-Z even-A fission products. Circles (green) indicate the $2^+ \rightarrow 0^+$ transition, squares (blue) indicate the $4^+ \rightarrow 2^+$ transition, and triangles (red) indicate a double-gate on both. The curves and points signify the mean correction over the three CGMF calculations (see text). The bands show the upper and lower correction values, where bands that have a lower bound of zero indicate that the particular γ-ray transition did not exist in the default RIPL-3 database.

to the assumed specifications (detector resolution, fission reaction, etc.), so a similar exercise should be conducted on an experiment-by-experiment basis.

The third correction is the multiplicity correction ϵ_M shown in Fig. 3, which accounts for the bias introduced by limiting the total number of γ rays used to identify a fission event. This is often used to improve the signal-to-noise ratio or ensure that γ rays are coincident with a fission event. In our analyses, we assume no ability to distinguish which fission product emitted the γ ray, a different approach than used previously [25]. Thus, our multiplicity cuts are for the total fission event. In Fig. 3, we note that a cut of $\nu_\gamma^T \geq 3$ has little effect, whereas a cut of $\nu_\gamma^T \geq 6$ requires a correction of about 80%, but there is considerable variance between the fission products and transitions. We note that we have not considered the detector efficiency here.

We determine ϵ_M by first masking on all CGMF events producing the target fission product. We apply a second mask to these sub-events that generate all target γ-ray transitions, so as not to double-count the level correction. We then determine the total number of γ rays emitted in these double-masked events and compare against potential cuts of $\nu_\gamma^T = 3, 6, 9$ γ rays. A notable result from this calculation, seen in Fig. 3, is that ϵ_M depends strongly on the fission product (i.e. a γ-ray multiplicity cut disproportionately affects certain fission products).

4 Results

Figure 4 illustrates the effect of utilizing these corrections. The (red) open squares show the inferred yields from a summation of the $4^+ \rightarrow 2^+$ transition photopeak over all CGMF events for each even-Z even-A fission product for ^{235}U($n_{\rm th}$, f). These results take into account the typical energy resolution of a Ge detector and utilize a $\nu_\gamma^T \geq 3$ multiplicity cut, a conservative estimate in Ge detector arrays not spanning a 4π solid angle [26]. The solid curve denotes the

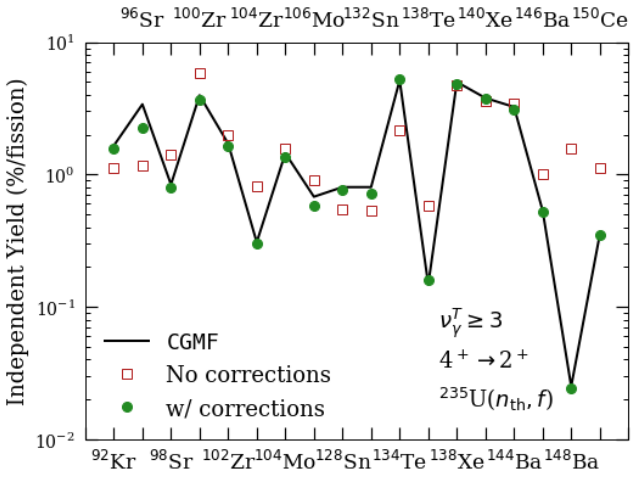

Figure 4. (Color online) Inferred yields for several even-Z even-A fission products from ^{235}U($n_{\rm th}$, f) using a single-gate on the $4^+ \rightarrow 2^+$ transition. Open (red) squares denote a simple photopeak area sum accounting for a typical [24] Ge detector resolution and a total γ-ray multiplicity cut of $\nu_\gamma^T \geq 3$. Closed (green) circles apply the average corrections over the three CGMF calculations (see text) to the photopeak sum results. The line shows the 'true' fission product yields sampled by CGMF.

'true' yields that comprise the sampling basis in Eq. 1. After applying the corrections

$$Y_{\rm corr}(A,Z) = Y_{\rm inf}(A,Z) \times \left(\frac{\epsilon_P}{\epsilon_L \epsilon_M}\right), \tag{4}$$

to the inferred yield $Y_{\rm inf}(A,Z)$, the (green) circles denote the corrected yields $Y_{\rm corr}(A,Z)$. The corrections ϵ_P, ϵ_L, and ϵ_M used in Fig. 4 are the average correction over the three CGMF calculations (i.e. the curves and points in Fig. 2 and Fig. 3).

We note that, for the most part, the corrected yields are closer to the 'true' yields by a significant margin and similar results were found for different transitions, fission reactions, and multiplicity cuts. A similar strategy was applied to GEANIE data for the ^{238}U(n=1.75 MeV, f) reaction [25]. The resulting yields were in reasonable agreement with inverse kinematics results [27].

5 Conclusion

We have outlined a procedure for calculating corrections to fission product yields inferred through γ-ray spectroscopy, a powerful but complex procedure. Three corrections were considered. The first results from including γ-ray transitions emitted from other fission products in an energy bin of a given detector. The second stems from the nuclear structure and distributions of excitation energy and spin of the generated fission products. The last considers implicit biases introduced by applying γ-ray multiplicity cuts. We used a Monte Carlo implementation of the statistical Hauser-Feshbach decay theory, the CGMF code, to infer the values of these corrections.

The corrections were found to improve the inferred yields from Doppler-corrected photopeak areas alone. We have calculated the value of these corrections and demonstrated their impact and variance with respect to model parameters. We emphasize that the exact values determined here incorporate a specific detector resolution and fission reaction. Thus, it will be important to conduct a similar analysis presented here for each detector setup and experiment.

This work was supported by the Office of Defense Nuclear Nonproliferation Research & Development (DNN R&D), National Nuclear Security Administration, US Department of Energy. It was performed under the auspices of the National Nuclear Security Administration of the US Department of Energy at Los Alamos National Laboratory under Contract DEAC52-06NA25396.

References

[1] I. Ahmad, W.R. Phillips, Reports on Progress in Physics **58**, 1415 (1995)

[2] J. Hamilton, A. Ramayya, S. Zhu, G. Ter-Akopian, Y. Oganessian, J. Cole, J. Rasmussen, M. Stoyer, Progress in Particle and Nuclear Physics **35**, 635 (1995)

[3] N. Fotiades, J.A. Cizewski, K.Y. Ding, R. Krücken, J.A. Becker, L.A. Bernstein, K. Hauschild, D.P. McNabb, W. Younes, P. Fallon et al., Physica Scripta **2000**, 127 (2000)

[4] A. Bogachev, L. Krupa, O. Dorvaux, E. Kozulin, M. Itkis, M.G. Porquet, A. Astier, D. Curien, I. Deloncle, G. Duchene et al., The European Physical Journal A **34**, 23 (2007)

[5] G.M. Ter-Akopian, J.H. Hamilton, Y.T. Oganessian, J. Kormicki, G.S. Popeko, A.V. Daniel, A.V. Ramayya, Q. Lu, K. Butler-Moore, W.C. Ma et al., Phys. Rev. Lett. **73**, 1477 (1994)

[6] S. Mukhopadhyay, L.S. Danu, D.C. Biswas, A. Goswami, P.N. Prashanth, L.A. Kinage, A. Chatterjee, R.K. Choudhury, Phys. Rev. C **85**, 064321 (2012)
[7] M. Gooden, C. Arnold, J. Becker, C. Bhatia, M. Bhike, E. Bond, T. Bredeweg, B. Fallin, M. Fowler, C. Howell et al., Nuclear Data Sheets **131**, 319 (2016), special Issue on Nuclear Reaction Data
[8] Krishichayan, M. Bhike, C.R. Howell, A.P. Tonchev, W. Tornow, Phys. Rev. C **100**, 014608 (2019)
[9] W. Hauser, H. Feshbach, Physical Review **87**, 366 (1952)
[10] P. Talou, T. Kawano, I. Stetcu, LA-CC-13063, Los Alamos Nat. Lab. (2013)
[11] B. Becker, P. Talou, T. Kawano, Y. Danon, I. Stetcu, Phys. Rev. C **87**, 014617 (2013)
[12] P. Jaffke, P. Möller, P. Talou, A.J. Sierk, Phys. Rev. C **97**, 034608 (2018)
[13] A.C. Wahl, Tech. rep., Los Alamos Nat. Lab. LA-13928 (2002)
[14] P. Möller, A. Sierk, T. Ichikawa, H. Sagawa, Atomic Data and Nuclear Data Tables **109-110**, 1 (2016)
[15] Vorobyev, A.S., Shcherbakov, O.A., Gagarski, A.M., Val'ski, G.V., Petrov, G.A., EPJ Web of Conferences **8**, 03004 (2010)
[16] A. Koning, J. Delaroche, Nuclear Physics A **713**, 231 (2003)
[17] J. Kopecky, M. Uhl, Phys. Rev. C **41**, 1941 (1990)
[18] R. Capote, M. Herman, P. Obložinskỳ, P. Young, S. Goriely, T. Belgya, A. Ignatyuk, A. Koning, S. Hilaire, V. Plujko et al., Nuclear Data Sheets **110**, 3107 (2009), special Issue on Nuclear Reaction Data
[19] A. Gilbert, A.G.W. Cameron, Canadian Journal of Physics **43**, 1446 (1965)
[20] A. Ignatyuk, K. Istekov, G. Smirenkin, Sov. J. Nucl. Phys.(Engl. Transl.);(United States) **29** (1979)
[21] E.Y. Yeoh, S.J. Zhu, J.H. Hamilton, A.V. Ramayya, Y.X. Liu, Y. Sun, J.K. Hwang, S.H. Liu, J.G. Wang, Y.X. Luo et al., Phys. Rev. C **82**, 027302 (2010)
[22] P. Lee, C.B. Moon, C.S. Lee, A. Odahara, R. Lozeva, A. Yagi, S. Nishimura, P. Doornenbal, G. Lorusso, P.A. Söderström et al., Phys. Rev. C **92**, 044320 (2015)
[23] W. Urban, K. Sieja, T. Rząca-Urban, M. Czerwiński, H. Naïdja, F. Nowacki, A.G. Smith, I. Ahmad, Phys. Rev. C **93**, 034326 (2016)
[24] A. Owens, Nuclear Instruments and Methods in Physics Research Section A: Accelerators, Spectrometers, Detectors and Associated Equipment **238**, 473 (1985)
[25] N. Fotiades, P. Casoli, P. Jaffke, M. Devlin, R.O. Nelson, T. Granier, P. Talou, T. Ethvignot, Phys. Rev. C **99**, 024606 (2019)
[26] J.N. Wilson, M. Lebois, L. Qi, P. Amador-Celdran, D. Bleuel, J.A. Briz, R. Carroll, W. Catford, H. De Witte, D.T. Doherty et al., Phys. Rev. Lett. **118**, 222501 (2017)
[27] D. Ramos, M. Caamaño, A. Lemasson, M. Rejmund, L. Audouin, H. Álvarez-Pol, J.D. Frankland, B. Fernández-Domínguez, E. Galiana-Baldó, J. Piot et al., Phys. Rev. Lett. **123**, 092503 (2019)